

Università degli studi di Padova

DEPARTMENT OF PHYSICS AND ASTRONOMY "GALILEO
GALILEI"

BACHELOR'S DEGREE IN ASTRONOMY

Selection of exoplanets in the habitable zone for atmospheric characterization with the James Webb Space Telescope

Supervisor:

Prof. Malavolta Luca

Candidate:

Semenzato Andrea

Accademic year 2022/2023

Abstract

The James Webb Space Telescope (JWST) is a powerful new tool that can be used for the atmospheric characterization of exoplanets, with unprecedented sensitivity and spectral resolution in the infrared. To select the best exoplanets for atmospheric characterization with JWST, we want to prioritize those in the habitable zone and for which we can obtain some atmospheric information through transmission or emission spectroscopy. In this thesis, according to specific metrics, I will present a selection algorithm for choosing exoplanets in the habitable zone that are optimal for atmospheric characterization with JWST. I will also apply this algorithm to a catalogue of known exoplanets to identify a list of priority targets for JWST observations.

Contents

Introduction	1
1 Exoplanet detection methods	3
1.1 Radial velocity	3
1.2 Transit	3
1.3 Direct imaging	4
1.4 Gravitational microlensing	4
2 James Webb Space Telescope	5
2.1 Instruments	5
2.2 Spectroscopy techniques	6
2.3 Fields of research	8
3 Study parameters	9
3.1 Stellar properties	9
3.2 Planetary properties	9
3.3 Goldilocks zone	10
3.4 TSM and ESM	11
4 Data elaboration	13
4.1 Dataset	13
4.2 Goldilocks zone filtering	14
4.3 TSM and ESM calculations	14
5 Python algorithm	16
6 Conclusions and discussions	22
List of Figures	25
Bibliography	27
Ringraziamenti	28

“The only rules are the ones dictated by the laws of physics.”
- Elon Musk

Introduction

The discovery of exoplanets stands as one of the greatest advancements in modern astronomical research. Since the confirmation of the first extrasolar planets by Mayor & Queloz (1995) and named "51 Pegasi b", over five thousand of exoplanets have been identified, a growing number of which are situated within the habitable zone of their respective stars, where conditions could be favorable for life development.

The James Webb Space Telescope, also known as JWST, is the most complex space telescope ever built; Thanks to its capability to observe the universe through an infrared band, the JWST is able to detect and examine exoplanets in a much more detailed way than was ever been possible to do with the previous models. .

The present thesis aims to present, analyze, and elaborate the information collected in the TEP-Cat Planetary Transits Database, which is a catalog resulting from the aggregation of the most relevant data of the scientific literature. The purpose of its drafting lies in the aspiration to provide a resume of the physics properties of the transiting exoplanets currently known. In the specific case of this analysis project, particular attention will be given to the group of exoplanets with the higher probability of having an atmosphere that can be analyzed in further context. Of the data proposed by the catalog, the following were selected:

Stellar properties:

- Effective Temperature ($^{\circ}\text{K}$).
- Radius (R_{\odot}).
- J-band magnitude (mj).
- k-band magnitude (mk).

Orbiting exoplanet properties:

- Equilibrium temperature ($^{\circ}\text{K}$).
- Radius (R_{\oplus}).
- Mass (M_{\oplus}).
- Semi-major axes (AU)

The thesis will be structured as follows: during the first chapter, it will delve into the subject of the most popular exoplanet detection methods. It will proceed, through the second chapter, towards a deeply detailed description of the James Webb Space Telescope and the relevance of the role it holds in the scientific field of modern astronomy. In the third chapter, the investigation will be centered on the series of necessary properties for an exoplanet to be found in the Goldilocks zone with a high probability of having developed a stable atmosphere.

In conclusion, in the fourth and final chapter of the work, the data elaborated with a Python algorithm will be presented with a list of the best candidates for further atmospheric spectroscopy analysis.

Chapter 1

Exoplanet detection methods

The quest to detect exoplanets employs a variety of methodologies. Among these, four primary methods are widely acknowledged within the astrophysical community for their effectiveness and reliability. This chapter offers an introductory exposition of these methods.

1.1 Radial velocity

The Radial Velocity method conceptualizes a Star-Planet system akin to a binary system with a single spectral signature. This approach hinges on the gravitational interaction between a star and its orbiting planet, which induces reciprocal stellar motion detectable through radial velocity shifts along the line of sight. Stellar displacement manifests as Doppler shifts in spectral lines - redshift when the star moves away and blueshift when it approaches the observer. This method's efficacy is contingent upon the orbital plane's inclination relative to our line of sight. A greater mass of the orbiting planet amplifies the gravitational influence on the star, intensifying the spectral line shift. This method is particularly effective for detecting planets in close orbits due to the inverse square law of gravitational force. However, its efficiency diminishes for planets with distant orbits, as prolonged observation periods become imperative.

1.2 Transit

The Transit method, a photometric technique, is predicated on observing the diminution in a star's brightness when a planet transits, or crosses in front of it. This method's efficacy is inherently linked to the rare occurrence of an orbital alignment that permits transits to be observable from Earth. The depth and duration of the light curve's dip are critical metrics in this analysis, correlating directly with the transiting planet's size and orbital period. Larger planets, such as gas giants, cause more significant dips in the star's brightness, making them easier to detect. However, the method also holds potential for identifying smaller, Earth-like planets, albeit with greater observational challenges. The periodic nature of these transits allows for the estimation of the planet's orbital period. By repeatedly observing these transits and analyzing the timing variations, astronomers can infer the presence of additional planets or moons influencing the transiting planet's orbit. The Transit method also facilitates the study of exoplanetary atmospheres. When a planet transits its star, some light filters through the planet's atmosphere, allowing astronomers to analyze the atmosphere's composition using spectroscopy. This analysis can reveal the presence of various gases, potentially including those indicative of biological processes. Additionally, the Transit method has been

instrumental in identifying multi-planet systems. Observations of multiple transit events, differing in depth and duration, suggest the presence of several planets in orbit around the same star. This aspect of the method has significantly contributed to our understanding of the diversity of planetary systems. Despite its strengths, the Transit method's reliance on specific orbital alignments means it observes only a fraction of the potential exoplanets. Moreover, the requirement for high-precision instrumentation to detect minute changes in stellar brightness limits its applicability from the ground to relatively bright and nearby stars. Missions like

1.3 Direct imaging

Direct Imaging technique endeavors to capture exoplanet's light, predominantly at infrared wavelengths where the luminosity disparity between a planet and its star is minimized. DI excels in accuracy, mitigating false positives prevalent in other methods. It enables the analysis of planetary atmospheric composition through spectral examination. However, its application is challenging due to the dimness of exoplanets and their proximity to bright stars. DI is thus restricted to a narrow subset of exoplanets, specifically those with wide orbits and substantial atmospheres or hot Jovians for their high luminosity in the infrared. Despite these limitations, DI offers unparalleled insights into exoplanetary atmospheres and potential habitability.

1.4 Gravitational microlensing

Gravitational Microlensing is a phenomenon predicted by Einstein's Theory of Relativity (1915) that involves the deflection and magnification of light from a distant star by a massive intervening object like a planet. This effect results in a detectable transient brightening of the star when the planet passes directly between the star and the observer. Principally used for detecting gas giants, the brightening effect is proportional to the intervening planet's mass and its distance from its host star. Microlensing is also applicable in detecting black holes and other massive celestial objects. Unlike other methods, the distance of the exoplanet from its star is not a limiting factor, allowing for the detection of orphan planets as well. However, a significant limitation of this technique is the difficulty in conducting follow-up observations for further characterization of the planet, as the transient nature of microlensing events often precludes repeated or detailed study of the same system.

Chapter 2

James Webb Space Telescope

The James Webb Space Telescope (JWST) represents a monumental leap in our capacity to observe the universe. Primarily operating in the infrared spectrum, the JWST is adept at exploring the farthest reaches of the cosmos, benefiting significantly from the redshift effect.

2.1 Instruments

The JWST's primary mirror, also called Optical Telescope Element (OTE), consists of 18 hexagonal beryllium segments assembled into a honeycomb structure. Each segment, measuring 1.4 meters across, is coated with a layer of gold 1000 Angstroms thick, optimizing the reflection of infrared radiation. An additional protective layer of amorphous SiO₂ shields these mirrors from scratches and potential impacts from space debris. The telescope features a primary concave mirror, a secondary convex mirror, and an off-center tertiary mirror, designed to correct astigmatism and flatten the focal plane, thereby eliminating aberrations and enabling wide-field imaging.

Integral to the JWST are four sophisticated instruments, each with distinctive features for state-of-the-art exoplanetary research:

- NIRCam (Rieke et al. (2005)): This near-infrared camera, equipped with a range of broadband, medium, and narrowband filters, is also capable of grism spectroscopy in the 0.6-5 μm range. Its coronagraphic capabilities are enhanced by a series of Lyot masks, allowing detailed observations of distant celestial bodies. (Figure 1; Krist et al. (2010)).
- NIRSpec (Ferruit et al. (2012)): As a versatile spectrograph, NIRSpec offers single, multi-object, and Integral Field (IFS) spectroscopy in the 0.7-5 μm range, with spectral resolutions between 100 and 3,000. This range and precision make it an invaluable tool for analyzing the composition of distant astronomical objects.
- MIRI (Rieke et al. (2015)): The Mid-Infrared Instrument (MIRI) is designed for direct imaging, slit and IFS spectroscopy at low and medium resolutions, and coronagraphy using fixed filters across 5.6 to 28.8 μm wavelengths. Its focal plane houses Three Four Quadrant Phase Masks and a Lyot coronagraph, facilitating detailed observations in mid-infrared ranges (Figure 1 Boccaletti et al. (2015)).
- NIRISS (Doyon et al. (2012)): This instrument offers broad capabilities in imaging and wide-field grism spectroscopy up to 5 μm , including aperture mask interferometry at 3.8 and 4.8 μm . It's a crucial tool for detailed examination of distant celestial phenomena.

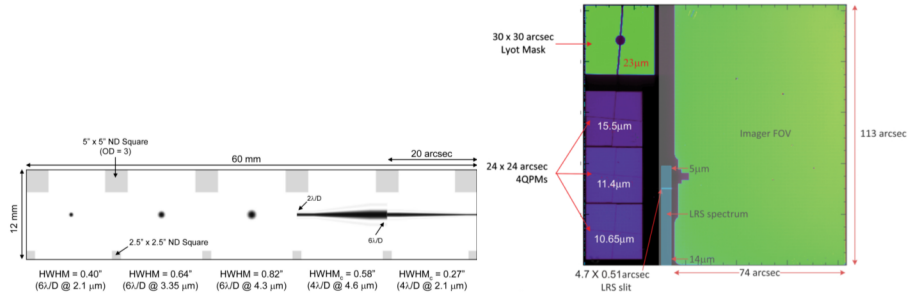


Figure 2.1: Left: NIRCcam has coronagraphic capabilities with a series of Lyot masks, including 3 circular and 2 wedge-shaped occulters optimized for different wavelengths; Right: MIRI focal plane has three Four Quadrant Phase Masks at 10.6, 11.4, 15.5 μm and a Lyot coronagraph at 23 μm (Beichman & Greene (2017)).

2.2 Spectroscopy techniques

The JWST predominantly utilizes the transit method for exoplanet detection, as elaborated in the previous chapter. Once detected, the exoplanet can be inspected with Transmission or Emission spectroscopy depending on the properties of the exoplanet. Transmission spectroscopy is a technique used to analyze the atmosphere of a transiting exoplanet. As the planet passes in front of its host star (a transit), some of the starlight filters through the planet's atmosphere. This process creates characteristic spectral lines in the starlight that can be detected and analyzed. These spectral lines can reveal the composition, temperature, and structure of the planet's atmosphere. The technique is most effective for planets with significant atmospheric scale heights and for host stars that are relatively bright in the visible and near-infrared wavelengths. Emission spectroscopy involves analyzing the light emitted directly by the planet itself, typically in the infrared wavelength range. This technique is particularly useful for studying the dayside temperatures and atmospheric composition of exoplanets. In emission spectroscopy, observations are often made during a secondary eclipse, when the planet passes behind its star, allowing the planet's emitted light to be isolated from the star's. One of the most significant discoveries of JWST is the independent confirmation of the exoplanet LHS475 b in August 2022 (Lustig-Yaeger et al. (2023)), a rocky planet nearly the size of Earth, orbiting the red dwarf star LHS475. This finding was significant, not just for the discovery itself, but for the capabilities it demonstrated in the JWST's instruments. The light curve analysis revealed the transit of LHS475 b, while spectroscopic data from NIRSpec suggested the potential atmospheric composition of the planet.

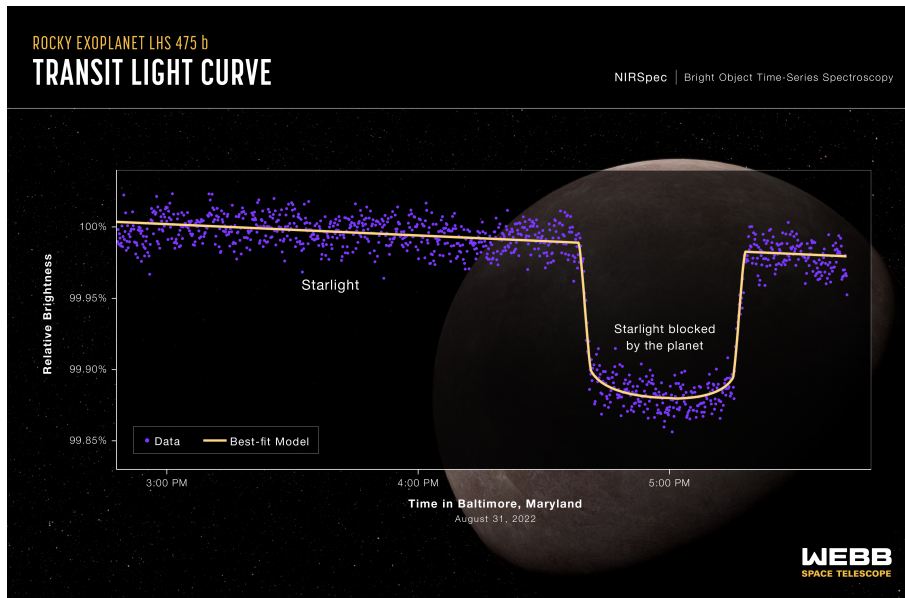


Figure 2.2: Light curve of LHS475 affected by the transit of LHS475 b. Credit: Illustration: NASA, ESA, CSA, L. Hustak (STScI); Science: K. Stevenson, J. Lustig-Yaeger, E. May (Johns Hopkins University Applied Physics Laboratory), G. Fu (Johns Hopkins University), e S. Moran (University of Arizona) ([Agosto,2022], NASA)

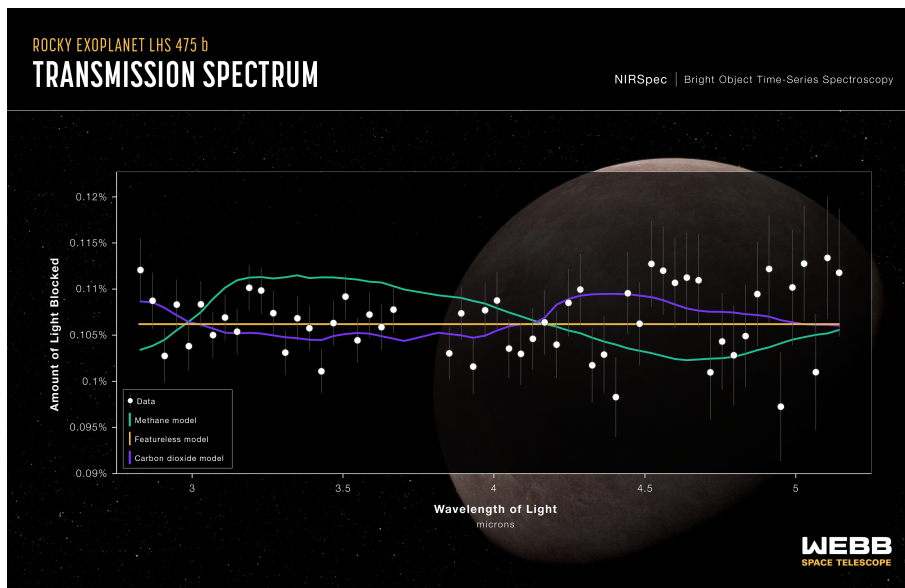


Figure 2.3: Transmission spectrum obtained using the NIRSpec (Near-Infrared Spectrograph) instrument; The data (white points) are consistent with a featureless spectrum representative of a planet without an atmosphere (yellow line); The purple line represents a pure carbon dioxide atmosphere and is indistinguishable from a flat line at the current level of precision; The green line represents a pure methane atmosphere, which is not favored because if methane were present, it would be expected to block more stellar light at 3.3 microns. Credit: Illustrazioni: NASA, ESA, CSA, L. Hustak (STScI); Science: K. Stevenson, J. Lustig-Yaeger, E. May (Johns Hopkins University Applied Physics Laboratory), G. Fu (Johns Hopkins University), e S. Moran (University of Arizona) ([Agosto,2022], NASA)

Mark Clampin, Director of the Astrophysics Division at NASA Headquarters, underscored the significance of these findings. He emphasized how the JWST is opening new avenues in understanding terrestrial planets beyond our solar system. The sensitivity of JWST’s instruments allows for detailed observations that could reveal a range of atmospheric molecules, though more observations are needed for conclusive evidence regarding the presence and composition of an atmosphere on LHS475 b.

2.3 Fields of research

While its capabilities in exoplanet detection are profound, the JWST's contributions extend far beyond, encompassing the study of primordial galaxies and other cosmic phenomena. Following, a brief introduction of some other fields of work.

Study of Primordial Galaxies: Galaxies that are formed shortly after the Big Bang, are shrouded in mystery and hold crucial information about the early universe. The JWST's advanced infrared capabilities allow it to peer back in time, capturing light from these ancient galaxies. This light has been stretched or 'redshifted' to longer wavelengths due to the expansion of the universe, making infrared observation essential. By studying these primordial galaxies, we could understand more about galaxy formation and evolution. The JWST's observations can reveal the physical conditions, composition, and dynamics of these early galaxies, offering insights into the processes that shaped the universe as it is.

Cosmic Structures and Dark Matter: By observing gravitational lensing effects, where the gravity of massive objects like galaxy clusters bends light from more distant galaxies, the JWST can help map the distribution of dark matter. These observations are crucial in understanding the role of dark matter in the structure and evolution of the universe.

Stellar and Planetary Formation: The telescope's infrared sensors can penetrate dense clouds of gas and dust, where stars and planets are born, providing unprecedented views of these cradles of celestial bodies. This can help scientists understand the conditions and processes that lead to star and planetary formation.

Cosmology and the Cosmic Microwave Background: While the JWST is not primarily designed to study the CMB, its observations can complement other missions focused on the CMB, enhancing our understanding of the early universe's conditions and the fundamental physics that governed its evolution.

Chapter 3

Study parameters

This chapter aims to elucidate the critical parameters for evaluating the potential of exoplanets to harbor atmospheres and reside within the habitable zone, commonly referred to as the 'Goldilocks zone'. These parameters are derived from the TEPCAT catalog, encompassing various physical and observational data of star-planet systems. Additionally, this chapter will explore the Transit Spectroscopy Metric (TSM) and Emission Spectroscopy Metric (ESM) (Kempton et al. (2018)), essential tools for identifying planets most likely to possess atmospheres.

3.1 Stellar properties

Effective temperature (T_{eff}):

The effective temperature of a star is a pivotal parameter in stellar astrophysics, providing a basis for classifying stars and inferring their properties such as luminosity and size. T_{eff} , indicative of a star's radiative energy output, is calculated using Wien's displacement law, establishing an inverse relationship between peak wavelength and temperature.

$$\lambda_{\text{max}} \cdot T = b \quad (3.1)$$

where λ_{max} is the peak emission wavelength, T is the temperature, and b is Wien's displacement constant.

Additionally, the Stefan-Boltzmann law relates a star's luminosity to T_{eff} , further underscoring its importance in understanding stellar characteristics and influencing the habitable zone's extent.

$$L = 4 \cdot \pi \cdot R^2 \cdot \sigma \cdot T_{\text{eff}}^4 \quad (3.2)$$

where L is the luminosity, R is the star's radius, and σ is the Stefan-Boltzmann constant. For exoplanetary studies, T_{eff} is crucial in determining the energy budget of orbiting planets, directly impacting their climate and habitability prospects. It also influences spectroscopic observations crucial for studying planetary atmospheres.

3.2 Planetary properties

Semi-major axes (a):

The semi-major axis, denoted as $a(\text{AU})$, is a fundamental parameter in celestial mechanics and exoplanet studies. It represents half the longest diameter of an elliptical orbit and is

critical in determining a planet's orbital period and its distance from the host star. According to Kepler's Third Law, the square of the orbital period (P) of a planet is directly proportional to the cube of the semi-major axis of its orbit:

$$P^2 = \frac{4\pi^2}{G(M + m)}a^3 \quad (3.3)$$

where P is the orbital period, G is the gravitational constant, M is the star's mass and m is the planet's mass.

In exoplanet studies, the semi-major axis is crucial for determining the amount of stellar radiation a planet receives, influencing its climate and potential habitability. For planets within the habitable zone, the semi-major axis helps in understanding the balance between being far enough from the star to avoid excessive heating and close enough to maintain adequate warmth for liquid water to exist.

Radius and Mass:

The radius and mass of an exoplanet are critical in determining its composition, atmosphere, and potential habitability. The radius gives an indication of the planet's size, which, when combined with mass, provides insights into its density and, therefore, its likely composition (whether it is a gas giant, a water world, or a rocky planet).

The relationship between a planet's radius and mass is complex and depends on its composition and internal structure. Generally, a planet's mass can be derived from its gravitational influence on nearby objects, including its host star or other planets, while its radius is often determined from transit observations. The mass-radius relationship can be expressed in a general form as:

$$M_p = \rho \cdot \frac{4\pi}{3} R_p^3 \quad (3.4)$$

where M_p is the planet's mass, R_p is the radius, and ρ is the average density of the planet. This equation, however, is an oversimplification with large errors derived from the difficulties of the measurements.

Understanding the mass-radius relationship is crucial for characterizing exoplanets. It allows researchers to estimate the composition of the planet and, by extension, its potential to host an atmosphere.

3.3 Goldilocks zone

The Goldilocks Zone, scientifically termed the habitable zone, refers to the region around a star where the conditions are just right (not too hot and not too cold) for liquid and gaseous water to exist on the surface and atmosphere of a planet. The existence of liquid water is considered a key ingredient for life as we know it, making the habitable zone a primary focus in the search for potentially habitable exoplanets.

The habitable zone's boundaries can be estimated using the concept of insolation $S_{\text{planet}}/S_{\oplus}$, which is the stellar energy a planet receives (S_{planet}) compared to what Earth receives from the Sun (S_{\oplus}).

The insolation parameter is calculated from the Luminosity also derived from 3.2:

$$S = \frac{L}{4\pi d^2} \quad (3.5)$$

According to Sullivan et al. (2015), a planet orbiting a solar-type star can be classified as residing within the habitable zone if the ratio of the stellar flux it receives to that which

Earth receives from the Sun lies within the range of $0.2 < S/S_{\oplus} < 2.0$. The parameters S_{outer} and S_{inner} delineate the outer and inner limits of the habitable zone, respectively. Further refinement in this definition was proposed by Kopparapu et al. (2013), who introduced a more stringent inner limit of $S/S_{\oplus} = 0.9$ for low-mass stars. This adjustment was driven by the recognition that smaller stars exhibit heightened activity in the ultraviolet (UV) and infrared (IR) spectra. Such activity implies that planets receiving a similar amount of total stellar irradiance as Earth might still be uninhabitable due to the differing spectral distribution of their stellar input. For this thesis, the inner limit of the habitable zone, S_{inner} , will be set at 1.05 times Earth's insolation as calculated by Leconte et al. (2013), who utilized sophisticated three-dimensional models that account for both radiative and convective emission and absorption in a self-consistent manner. Having established these insolation-based boundaries, it is then possible to translate these limits into distances, expressed in Astronomical Units (AU).

$$d_{inner} = \sqrt{\frac{1}{S_{outer}}} \qquad d_{outer} = \sqrt{\frac{1}{S_{inner}}} \qquad (3.6)$$

where d_{inner} and d_{outer} are the distances from the star to the inner and outer edges of the habitable zone, respectively, measured in astronomical units (AU).

Planets within this zone are prime candidates for further studies, particularly in assessing their atmospheric properties and surface conditions.

3.4 TSM and ESM

The TSM is designed to quantify the feasibility of conducting transmission spectroscopy on transiting exoplanets. It is a measure of the expected signal-to-noise ratio (S/N) for transmission spectroscopic observations, taking into account factors like the planet's atmospheric scale height, its radius, and the brightness of the host star. The TSM is particularly useful for prioritizing planets for atmospheric characterization, especially for those in the Neptune (to Earth)-size range. TSM is most applicable for planets with clear atmospheres and those orbiting bright stars, as these conditions optimize the detection of spectral features.

According to Kempton et al. (2018), the TSM is determined by considering several factors:

- The strength of the spectral features, depends on the atmospheric scale height.
- The radius of the planet (R_p).
- The equilibrium temperature of the planet (T_{eq}).
- The mass of the planet (M_p).
- The radius of the host star (R_{\star}).
- The apparent magnitude of the host star in the J band (m_J).

The TSM is given by the formula:

$$TSM = (\text{Scale factor}) \times \frac{R_p^3}{M_p} \times \frac{T_{eq}}{R_{\star}^2} \times 10^{-m_J/5} \qquad (3.7)$$

where, if not already given by the TEPcat, the equilibrium temperature can be calculated

utilizing the following equation:

$$T_{eq} = T_* \sqrt{\frac{R_*}{2a}} \quad (3.8)$$

where T_{eq} the planet's equilibrium temperature in Kelvin calculated for zero albedo and full day-night heat redistribution. For this study, a good TSM value for Neptunian-size exoplanets is set to be > 10 .

The ESM is a calculated metric for assessing the expected S/N for emission spectroscopy observations of exoplanets (Kempton et al. (2018)), particularly at mid-infrared wavelengths. It is especially useful for studying terrestrial planets within the habitable zone. The ESM takes into account the planet's dayside temperature, its radius, and the brightness of the host star in the K-band. It is particularly relevant for JWST secondary eclipse observations. The ESM formula is represented as:

$$ESM = 4.29 \times 10^6 \times \frac{B(T_{day}, 7.5\mu m)}{B(T_*, 7.5\mu m)} \times \left(\frac{R_p}{R_*}\right)^2 \times 10^{-m_K/5} \quad (3.9)$$

Here, $B(T_{day}, 7.5\mu m)$ denotes Planck's function for the planet's dayside temperature evaluated at $\lambda = 7.5 \mu m$ while $B(T_*, 7.5\mu m)$ and the scale factor ensures the metric is aligned with expected S/N values for JWST secondary eclipse observations.

For this study, a good ESM value for Earth-size exoplanet is set to be > 7.5 .

Both TSM and ESM are fundamental parameters that guide the selection of exoplanets for atmospheric characterization, especially with JWST and other large telescopes, by providing a standardized approach to evaluate the potential of different exoplanets based on their observable characteristics.

Chapter 4

Data elaboration

This chapter embarks on a comprehensive analysis and interpretation of exoplanet systems, elaborating data from the TEPCCat catalog, as outlined in earlier sections.

The approach to this analysis is structured in two phases: the initial phase involves refining the dataset to isolate only those systems residing within the Goldilocks zone; The next step entails the computation of Transmission Spectroscopic Metric (TSM) and Emission Spectroscopic Metric (ESM) values for these selected systems.

4.1 Dataset

The dataset comprises a range of critical parameters pertaining to exoplanets and their host stars, which are essential for our research objectives. These parameters are systematically presented in the following table:

System	a [AU]	R_A [R_\odot]	T_{eff} [K]	M_b [M_\oplus]	R_b [R_\oplus]	T_{eq} [K]	Kmag	Jmag
55_Cnc_e	0.02	0.95	5172	7.72	1.90	2349.0	4.01	4.77
pi_Men_c	0.07	1.19	5998	3.62	2.15	1170.0	4.24	4.87
AU_Mic_b	0.08	0.75	3700	38.14	5.12	570.0	4.53	5.44
AU_Mic_c	0.14	0.75	3700	31.78	3.14	436.0	4.53	5.44
CoRoT-01	0.03	1.13	5950	327.33	17.39	1915.0	12.15	12.46

Table 4.1: The table presented here shows the first 5 lines of the new dataset, a refined version of the original one. This dataset has been specifically created to include only those parameters that are crucial for defining the Goldilocks zone and calculating the TSM and ESM. For a comprehensive view of all the data available in the catalog: <https://www.astro.keele.ac.uk/jkt/tepcat/>

The table comprises 1,225 systems, each curated to ensure completeness. For systems lacking information on the planet's mass or equilibrium temperature, missing data were supplemented. The planetary masses were sourced from the NASA Exoplanet Catalog, a reputable repository for exoplanetary data. As for the equilibrium temperatures, these were calculated with the equation (3.8) mentioned before.

4.2 Goldilocks zone filtering

The primary objective of this section is to calculate the luminosity for each exoplanet system and subsequently compute its insolation values. This process is fundamental to identifying planets that reside within the habitable zone.

The luminosity calculation involves applying the 3.2. Applying this formula constructs a comprehensive dictionary containing the luminosity of each star in the dataset. Once luminosities are obtained, the next step is to calculate the insolation, defined in eq. 3.5, representing the amount of stellar energy received per unit area on a planet. The approach is to apply the insolation formula to each system, considering the luminosity of the host star and the orbital distance of the planet. An aspect of this analysis is comparing these insolation values with that of Earth (denoted as S_{\oplus}). This comparison provides a relative scale to assess whether a planet receives more, less, or similar amounts of stellar energy compared to Earth. The final step in this section is to filter the systems based on their insolation values. The criteria this thesis adopts are not so stringent - only considering systems where the insolation value is between 0.2 and 1.05 times that of Earth's ($0.2 < S/S_{\oplus} < 1.05$). Upon applying these filtering criteria, a refined dataset is obtained.

System	T_{eff} [K]	R_A [R_{\odot}]	T_{eq} [K]	R_b [R_{\oplus}]	M_b [M_{\oplus}]	a [AU]	Jmag	Kmag	S/S_{\oplus}
Kepler-016	4450	0.65	185.00	8.45	105.83	0.70	9.82	9.00	0.30
Kepler-047c	5636	0.94	267.82	4.65	3.18	0.96	13.97	13.54	0.87
Kepler-150f	5560	0.94	233.31	3.64	12.90	1.24	13.82	13.36	0.49
Kepler-186f	3852	0.47	213.88	1.17	1.24	0.36	12.47	11.61	0.34
Kepler-296f	3740	0.48	247.43	1.80	3.89	0.26	13.39	12.60	0.60
Kepler-421	5308	0.76	185.00	4.16	16.10	1.22	12.01	11.54	0.28
Kepler-441b	4340	0.55	194.00	1.64	3.33	0.64	13.04	12.29	0.24
Kepler-442b	4402	0.60	256.67	1.35	2.30	0.41	13.23	12.49	0.72
Kepler-443b	4723	0.71	271.99	2.33	6.04	0.50	14.36	13.81	0.90
Kepler-1647	6210	1.79	242.92	11.87	483.06	2.72	12.38	12.01	0.58
Kepler-1654	5597	1.18	206.00	9.18	158.90	2.03	12.28	11.92	0.30
Kepler-1661	5100	0.76	269.82	3.87	16.84	0.63	12.73	12.16	0.89
Kepler-1704	5772	1.70	254.00	11.94	1318.87	2.03	12.14	11.79	0.70
LHS_1140b	3216	0.21	379.00	1.64	6.39	0.10	9.61	8.82	0.43
TOI-700d	3459	0.42	269.00	1.07	1.25	0.16	9.47	8.63	0.89
TOI-715	3075	0.24	234.00	1.44	1.55	0.08	11.81	10.92	0.73
TOI-2257	3430	0.31	256.00	2.20	5.72	0.14	11.47	10.67	0.61
TRAPPIST-1e	2566	0.12	246.10	0.92	0.70	0.03	11.35	10.30	0.63
TRAPPIST-1f	2566	0.12	214.50	1.04	1.05	0.04	11.35	10.30	0.35
TRAPPIST-1g	2566	0.12	194.50	1.13	1.33	0.05	11.35	10.30	0.23
K2-072e	3497	0.23	259.45	0.82	2.21	0.10	11.68	10.96	0.71

Table 4.2: The table presented showcases the data that has been selectively filtered to include only those systems within their respective habitable zones.

The final table reveals 20 systems aligning with the goal, now highlighted as prime candidates for the next step of the analysis.

4.3 TSM and ESM calculations

In this stage of the analysis, the focus shifts to quantifying the Transmission Spectroscopic Metric (TSM) and Emission Spectroscopic Metric (ESM) for each system within the habitable

zone. This work is fundamental in assessing the potential for atmospheric characterization of these exoplanets. The process begins with the application of equations 3.7 and 3.9, which provide the formulas for calculating TSM and ESM, respectively. Once the TSM and ESM values are computed for each system, these metrics are seamlessly integrated into our dataset. This integration is achieved by adding new columns to our existing table, explicitly dedicated to displaying the TSM and ESM values for each system. To further refine the analysis, it is important to establish specific thresholds for what constitutes 'good' TSM and ESM values. A system is considered to have a favorable TSM if its value exceeds 10 for $R_p < 1.5 R_\odot$ and 90 for $1.5 < R_p < 10 R_\odot$, indicative of a high potential for successful transmission spectroscopy. Similarly, an ESM value greater than 7.5 is deemed favorable for rocky planets, suggesting a high likelihood of obtaining meaningful emission spectroscopy data. The last phase of filtering involves isolating those systems within the habitable zone that also meet our defined standards and creating two tables with the results. Upon filtering systems with a favorable ESM value, it is observed that none of the systems in the initial dataset simultaneously meet both conditions established in this study. The rationale behind these findings will be discussed in Chapter 6.

System	T_{eff} [K]	R_A [R_\odot]	T_{eq} [K]	R_b [R_\oplus]	M_b [M_\oplus]	a [AU]	Jmag	Kmag	S/S_\oplus	TSM
TRAPPIST-1e	2566	0.12	246.1	0.92	0.70	0.03	11.35	10.3	0.63	19.40
TRAPPIST-1f	2566	0.12	214.5	1.04	1.05	0.04	11.35	10.3	0.35	16.28
TRAPPIST-1g	2566	0.12	194.5	1.13	1.33	0.05	11.35	10.3	0.23	14.95

Table 4.3: Systems in the habitable zone with good TSM values.

This final table not only highlights systems within the habitable zone but also emphasizes those with promising TSM values. This dual-focus approach allows to pinpoint the most promising candidates for further spectroscopic analysis and study, particularly in the context of atmospheric analysis and the search for life-supporting conditions.

Chapter 5

Python algorithm

```
1  #!/usr/bin/env python
2  # coding: utf-8
3
4  # In[1]:
5
6
7  #Librerie
8  import math
9  import pandas as pd
10 import numpy as np
11
12
13 # In[2]:
14
15
16 # Dataset
17 # Loading the modified csv (I removed zeros, unnecessary
18   # columns, and changed the unit of measurement
19   # for planets (from Jovian units to Terrestrial units))
20 data_df = pd.read_csv("data.csv")
21
22 # Checking the total number of systems remaining in the
23   # analysis
24 number_of_systems = data_df['System'].nunique()
25 print(number_of_systems)
26
27 # I notice that in the dataset there are negative values (-1)
28   # due to the csv export from the catalog.
29 # These values correspond to the mass of the planets and their
30   # equilibrium temperature.
31 # I search for updated mass values in the scientific literature
32   # and replace the value in the
33   # dataset (I do this only for systems promising for the purpose
34   # of the thesis).
35 # Creating a dictionary of the systems with the new mass
36 new_masses = {
37     'Kepler-186f': 1.24, #NASA
38     'Kepler-442b': 2.3, #NASA
39     'TOI-700d': 1.25, #NASA
```

```

34     'TOI-715': 1.55, #Monthly Notices of the Royal Astronomical
        Society
35     'K2-072e': 2.21, #NASA
36     'Kepler-150f': 12.9, #NASA
37     'Kepler-296f': 3.89, #NASA
38     'Kepler-441b': 3.33, #NASA
39     'Kepler-421': 16.1, #NASA
40     'Kepler-1654': 158.9, #NASA
41     'K2-155d': 4.27, #NASA
42     'Kepler-069c': 4.91, #Estimation of mass-radius
43     'Kepler-296e': 2.96, #NASA
44     'Kepler-436b': 7.9, #NASA
45     'Kepler-438b': 1.46, #NASA
46     'Kepler-439b': 5.65, #NASA
47     'Kepler-440b': 4.12, #NASA
48     'Kepler-443b': 6.04, #NASA
49     'TOI-700e': 0.818, #NASA
50     'TOI-712d': 6.68, #NASA
51     'K2-009b': 5.69, #NASA
52     'K2-072c': 1.65, #NASA
53 }
54
55 # Updating the planetary mass values of systems with negative
    mass in the DataFrame.
56 for system_name, new_mass in new_masses.items():
57     data_df.loc[data_df['System'] == system_name, 'M_b'] =
        new_mass
58
59 # For the negative equilibrium temperature values, I calculate
    it using the already known equation
60 # making sure to convert both the radius of the star and the
    semi-major axis into meters.
61 def calculate_teq(T_star, R_star, a):
62     # Ensuring float values.
63     T_star = float(T_star)
64     R_star = float(R_star)
65     a = float(a)
66     # Calculating Teq
67     Teq = T_star * ((R_star*6.957e5 / (a*1.496e8)) ** 0.5) *
        ((1 / 4) ** 0.25)
68     return Teq
69
70 # Applying the function to the rows that have Teq == -1 in the
    data_df DataFrame
71 data_df.loc[data_df['Teq'] == -1, 'Teq'] = data_df.apply(
72     lambda row: calculate_teq(row['Teff'], row['R_A'], row['a(
        AU)']) if row['Teq'] == -1 else row['Teq'],
73     axis=1)
74
75 # Rounding the DataFrame to two decimal places.
76 data_df = data_df.round(2)
77 # Printing the first 5 systems with their parameters to see if
    everything is fine.

```

```

78 print(data_df.head())
79
80
81 # In[3]:
82
83
84 # Goldilocks Zone
85 # Defining the constants
86 sigma = 5.670374419e-8 # Stefan-Boltzmann constant [W/m^2/K^4]
87 earth_insolation = 1361 # Earth's insolation constant [W/m^2]
88
89 # To calculate the insolation, I need the Luminosity (L). I
    calculate it using the effective temperature
90 # of the star (Teff) and the radius of the star (R_A). R_A is
    measured in solar radii so
91 # I multiply by the sun's radius to convert it into meters
    (6.957e8 meters).
92 data_df['L'] = 4 * np.pi * ((data_df['R_A'] * 6.957e8)) ** 2 *
    sigma * (data_df['Teff'] ** 4)
93
94 # Calculating the insolation received by each planet using a(AU
    ) which is the semi-major axis in
95 # astronomical units (so I need to multiply it by 1.496e11
    meters).
96 data_df['S'] = data_df['L'] / (4 * np.pi * (data_df['a(AU)'] *
    1.496e11) ** 2)
97
98 # Calculating the insolation in terms of Earth's insolation by
    dividing by the constant (S $\oplus$ ).
99 data_df['S/S $\oplus$ '] = data_df['S'] / earth_insolation
100
101 # Describing the habitable zone limits from insolation. The
    habitable zone is defined by
102 # an outer limit of 0.2 and an inner limit of 1.05 times that
    of Earth according to Leconte (2013).
103 data_df['HZ'] = data_df['S/S $\oplus$ '].between(0.2, 1.05)
104
105 # Filtering only the systems within the habitable zone.
106 habitable_zone_systems = data_df[data_df['HZ']].copy()
107
108 # Selecting only the columns I want to show in the final table.
109 columns_of_interest = ['System', 'Teff', 'R_A', 'Teq', 'R_b', '
    M_b', 'a(AU)', 'Jmag', 'Kmag', 'S/S $\oplus$ ']
110
111 # Creating the table with the collected data and rounding the
    values to two decimal places.
112 habitable_zone_table = habitable_zone_systems[
    columns_of_interest]
113 habitable_zone_table = habitable_zone_table.round(2)
114
115 # Checking how many objects there are.
116 number_of_lines_habitable_zone = len(habitable_zone_table)
117 print(number_of_lines_habitable_zone)

```



```

118
119 # Displaying the table.
120 pd.set_option('display.width', 1000)
121 print(habitable_zone_table)
122
123
124 # In[4]:
125
126
127 # TSM and ESM
128 # Defining the scale factor for TSM
129 Rt = 1
130 def calculate_scale_factor(Rp, Rt):
131     if Rp < 1.5 * Rt:
132         return 0.190
133     elif 1.5 * Rt <= Rp < 2.75 * Rt:
134         return 1.26
135     elif 2.75 * Rt <= Rp < 4.0 * Rt:
136         return 1.28
137     elif 4.0 * Rt <= Rp < 10 * Rt:
138         return 1.15
139     else:
140         return None
141
142 # Defining the function for TSM.
143 def calculate_TSM(row):
144     scale_factor = calculate_scale_factor(row['R_b'], Rt)
145     if scale_factor is None:
146         return None
147     TSM = scale_factor * (((row['R_b'])**3) *
148                          (row['Teq'])) / ((row['M_b'] * ((row
149                          ['R_A'])**2))) *
150                          10**(-0.2 * row['Jmag']))
151     return TSM
152 # Defining Planck function for ESM
153 def planck_function(T):
154     # Constants for Planck's law.
155     h = 6.626e-34 # Planck's constant (m^2 kg / s)
156     c = 299792458 # Speed of light (m / s)
157     k = 1.381e-23 # Boltzmann's constant (m^2 kg / s^2 / K)
158     λ = 7.5e-6 # Wavelength at 7.5 micrometers
159     # Defining the law.
160     B_λ = ((2 * h * c**2) / (λ**5)) * 1 / (np.exp((h * c) / (λ
161     * k * T)) - 1)
162     return B_λ
163
164 # Defining Tday for ESM
165 def calculate_Tday(Teq):
166     Tday = 1.1 * Teq
167     return Tday
168
169 # Define the ESM calculation function using the actual equation
170 from the PDF

```

```

168 def calculate_ESM(row):
169     Tday = calculate_Tday(row['Teq'])
170     B7_5_Tday = planck_function(Tday)
171     B7_5_Tstar = planck_function(row['Teff'])
172     ESM = 4.29*1e6*(B7_5_Tday / B7_5_Tstar)*((row['R_b'])/((row
173         ['R_A']*109)))**2*10**(-0.2*row['Kmag'])
174     return ESM
175
176 # Define the columns of interest (assuming 'columns_of_interest
177     ' was defined earlier)
178
179 columns_of_interest_with_tsm = columns_of_interest + ['TSM']
180 columns_of_interest_with_esm = columns_of_interest + ['ESM']
181
182 # Now we can safely apply the TSM and ESM calculations to the
183     habitable_zone_systems DataFrame
184 habitable_zone_systems.loc[:, 'TSM'] = habitable_zone_systems.
185     apply(calculate_TSM, axis=1)
186 habitable_zone_systems.loc[:, 'ESM'] = habitable_zone_systems.
187     apply(calculate_ESM, axis=1)
188
189 # Create the habitable_zone_table with the new columns
190     including TSM and ESM
191 final_habitable_zone_table_tsm = habitable_zone_systems[
192     columns_of_interest_with_tsm]
193 final_habitable_zone_table_esm = habitable_zone_systems[
194     columns_of_interest_with_esm]
195
196 # Rounding
197 final_habitable_zone_table_tsm = final_habitable_zone_table_tsm
198     .round(2)
199 final_habitable_zone_table_esm = final_habitable_zone_table_esm
200     .round(2)
201
202 # Display the head of the updated tables
203 print('Systems with TSM')
204 print(final_habitable_zone_table_tsm)
205 print()
206 print('Systems with ESM')
207 print(final_habitable_zone_table_esm)
208
209 # In[5]:
210
211 # Final Considerations for the Best Set of Planets
212 # I want to find the best candidates from both tables. I need
213     criteria to determine when I have a
214     # good value of TSM and when of ESM.
215
216 # Filter for "good TSM" values
217 good_tsm_systems = final_habitable_zone_table_tsm[
218     ((final_habitable_zone_table_tsm['R_b'] < 1.5) & (
219         final_habitable_zone_table_tsm['TSM'] > 10)) |

```

```
209     ((final_habitable_zone_table_tsm['R_b'] >= 1.5) & (
210         final_habitable_zone_table_tsm['R_b'] < 10) & (
211         final_habitable_zone_table_tsm['TSM'] > 90))
212 ]
213 # Filter for "good ESM" values for terrestrial planets
214 good_esm_systems = final_habitable_zone_table_esm[
215     (final_habitable_zone_table_esm['ESM'] > 7.5)]
216 # Rounding
217 good_tsm_systems = good_tsm_systems.round(2)
218 good_esm_systems = good_esm_systems.round(2)
219
220 # Print the well-formatted tables
221 print("Good TSM Systems Table:")
222 print(good_tsm_systems)
223 print("\nGood ESM Systems Table:")
224 print(good_esm_systems)
```

Chapter 6

Conclusions and discussions

This chapter aims to analyze the results' validity and informative value of this thesis. The first point of discussion is the reason behind the lack of systems with a sufficient ESM value in the habitable zone. To identify such systems, it is necessary to consider Jovian planets orbiting close to low-mass stars and not in the Goldilocks zone, whose limits are defined by Leconte et al. (2013). This is because the larger the ratio of the planet's radius to the star's radius, the greater its contribution to the ESM value (3.9). For rocky planets in the habitable zone, which are typically farther from their host star, the reflected light from the planet is less.

Table 6.1 depicts the ESM values for all systems listed in the TEPcat, within the habitable zone.

A notable correlation emerges regarding the solar radius; it is observed that the stars hosting planets within their habitable zone have radii ranging from 0.12 to 1.79 solar radii, with a median of 0.55 and a standard deviation of 0.46. This observation indicates that stars hosting planets in the habitable zone are predominantly low-mass stars rather than solar-type stars. This can be attributed to two factors: First, detecting planets orbiting smaller stars is more feasible using the transit method. In this scenario, the planet's relative size compared to a smaller star causes a more significant reduction in the star's light curve during transit, improving the likelihood of detection. Second, for planets orbiting close to their host star to be classified within the habitable zone, they must orbit smaller stars. This requirement is due to smaller stars having lower luminosity, which allows a planet in a closer orbit to maintain conditions that could support habitability.

Furthermore, the equilibrium temperatures of the planets in question vary from 180 K to 380 K, with a median equal to 246.10 and a standard deviation of 41.85. Planets included in the final dataset, particularly those with temperatures in the lower range, may experience heating effects attributable to containment mechanisms, likely due to the presence of an atmosphere. This atmospheric layer can act as an insulator, trapping heat and potentially warming the planet, as the greenhouse effect does with Earth and Venus. This consideration is pivotal when addressing the habitability of planets that are colder and farther from their host star. As described by Kopparapu (2013), systems with an insolation ratio $S/S_{\oplus} = 0.2$ may still be deemed habitable if they possess an atmosphere, due to the so-called "moist greenhouse effect". This effect refers to a climatic scenario in which the stratosphere becomes dominated by water vapor. This leads to a rapid escape of hydrogen into space, significantly affecting the planet's atmospheric composition and climate. In such conditions, even with reduced solar energy (as indicated by an insolation ratio of 0.2), a planet can maintain liquid water on its surface, a key criterion for habitability. This effect relies on a dense water vapor atmosphere,

System	T _{eff}	R _A	T _{eq}	R _b	M _b	a(AU)	J _{mag}	K _{mag}	S/S _⊕	ESM
Kepler-016	4450	0.65	185.00	8.45	105.83	0.70	9.82	9.00	0.30	0.04
Kepler-047c	5636	0.94	267.82	4.65	3.18	0.96	13.97	13.54	0.87	0.01
Kepler-150f	5560	0.94	233.31	3.64	12.90	1.24	13.82	13.36	0.49	0.00
Kepler-186f	3852	0.47	213.88	1.17	1.24	0.36	12.47	11.61	0.34	0.00
Kepler-296f	3740	0.48	247.43	1.80	3.89	0.26	13.39	12.60	0.60	0.01
Kepler-421	5308	0.76	185.00	4.16	16.10	1.22	12.01	11.54	0.28	0.00
Kepler-441b	4340	0.55	194.00	1.64	3.33	0.64	13.04	12.29	0.24	0.00
Kepler-442b	4402	0.60	256.67	1.35	2.30	0.41	13.23	12.49	0.72	0.00
Kepler-443b	4723	0.71	271.99	2.33	6.04	0.50	14.36	13.81	0.90	0.01
Kepler-1647	6210	1.79	242.92	11.87	483.06	2.72	12.38	12.01	0.58	0.02
Kepler-1654	5597	1.18	206.00	9.18	158.90	2.03	12.28	11.92	0.30	0.01
Kepler-1661	5100	0.76	269.82	3.87	16.84	0.63	12.73	12.16	0.89	0.02
Kepler-1704	5772	1.70	254.00	11.94	1318.87	2.03	12.14	11.79	0.70	0.03
LHS_1140b	3216	0.21	379.00	1.64	6.39	0.10	9.61	8.82	0.43	3.14
TOI-700d	3459	0.42	269.00	1.07	1.25	0.16	9.47	8.63	0.89	0.05
TOI-715	3075	0.24	234.00	1.44	1.55	0.08	11.81	10.92	0.73	0.04
TOI-2257	3430	0.31	256.00	2.20	5.72	0.14	11.47	10.67	0.61	0.11
TRAPPIST-1e	2566	0.12	246.10	0.92	0.70	0.03	11.35	10.30	0.63	0.17
TRAPPIST-1f	2566	0.12	214.50	1.04	1.05	0.04	11.35	10.30	0.35	0.08
TRAPPIST-1g	2566	0.12	194.50	1.13	1.33	0.05	11.35	10.30	0.23	0.04
K2-072e	3497	0.23	259.45	0.82	2.21	0.10	11.68	10.96	0.71	0.03

Table 6.1: Systems in the habitable zone with their calculated ESM values. As anticipated, planets with the same radius as Earth, orbiting at distances close to one astronomical unit, exhibit significantly lower ESM values.

as demonstrated in empirical studies, where higher surface temperatures (for instance, 400 K) and specific atmospheric compositions (like a background gas of 4 bar of N₂ and a total surface pressure of 6.5 bar) result in different outgoing infrared (IR) radiation patterns compared to standard models. These patterns are crucial in understanding the radiation balance and, consequently, the potential for habitable conditions on such planets.

It is noteworthy that the best "Earth-like" candidate identified is TRAPPIST-1e, first discovered by Gillon et al. (2017). This exoplanet has been extensively studied by Krissansen-Totton et al. (2018) and colleagues, who emphasize its potential to host detectable biosignatures in anoxic atmospheres, a key indicator of life. Their research focuses on the possibility of detecting disequilibrium biosignatures, particularly the methane and carbon dioxide combination, using the James Webb Space Telescope. These observations could be achieved with few transits, offering a 90% confidence level. TRAPPIST-1e's Earth-like size, temperature, and potentially habitable conditions, combined with its location in the habitable zone and proximity to Earth, make it an ideal candidate for further exploration, both through telescopic studies and potential future space missions.

A special mention must be given to the LHS 1140 b system (ESM = 3.14), which is garnering increasing interest in the scientific community. This system, as described in the article published by Wunderlich, Fabian et al. (2021), could hold a hydrogen-dominated atmosphere and is an excellent candidate for detecting atmospheric features. The study investigated how the insolation and planetary parameters influence the atmospheric climate chemistry and spectral appearance of LHS 1140 b. They used the 1D-TERRA model to simulate a range of atmospheric compositions dominated by molecular hydrogen (H₂) and carbon dioxide (CO₂),

also varying methane (CH_4) concentrations. The research revealed that in H_2 -dominated and CH_4 -rich atmospheres, potential biosignatures like NH_3 , PH_3 , CH_3Cl , and N_2O are less sensitive to H_2 , CO_2 , and CH_4 concentrations. If LHS 1140 b indeed has a thin, clear hydrogen-dominated atmosphere, it could become a prime target for detecting biosignature gases in the atmosphere of a habitable-zone rocky exoplanet using the JWST and ELT

List of Figures

2.1	Left: NIRCcam has coronagraphic capabilities with a series of Lyot masks, including 3 circular and 2 wedge-shaped occulters optimized for different wavelengths; Right: MIRI focal plane has three Four Quadrant Phase Masks at 10.6, 11.4, 15.5 μm and a Lyot coronagraph at 23 μm (Beichman & Greene (2017)).	6
2.2	Light curve of LHS475 affected by the transit of LHS475 b. Credit: Illustration: NASA, ESA, CSA, L. Hustak (STScI); Science: K. Stevenson, J. Lustig-Yaeger, E. May (Johns Hopkins University Applied Physics Laboratory), G. Fu (Johns Hopkins University), e S. Moran (University of Arizona) ([Agosto,2022], NASA)	7
2.3	Transmission spectrum obtained using the NIRSspec (Near-Infrared Spectrograph) instrument; The data (white points) are consistent with a featureless spectrum representative of a planet without an atmosphere (yellow line); The purple line represents a pure carbon dioxide atmosphere and is indistinguishable from a flat line at the current level of precision; The green line represents a pure methane atmosphere, which is not favored because if methane were present, it would be expected to block more stellar light at 3.3 microns. Credit: Illustrazioni: NASA, ESA, CSA, L. Hustak (STScI); Science: K. Stevenson, J. Lustig-Yaeger, E. May (Johns Hopkins University Applied Physics Laboratory), G. Fu (Johns Hopkins University), e S. Moran (University of Arizona) ([Agosto,2022], NASA)	7

Bibliography

- Beichman, C. A. & Greene, T. P. 2017, *Observing Exoplanets with the James Webb Space Telescope*, ed. H. J. Deeg & J. A. Belmonte (Cham: Springer International Publishing), 1–26
- Boccaletti, A., Lagage, P.-O., Baudoz, P., et al. 2015, *Publications of the Astronomical Society of the Pacific*, 127, 633
- Doyon, R., Hutchings, J. B., Beaulieu, M., et al. 2012, in *Space Telescopes and Instrumentation 2012: Optical, Infrared, and Millimeter Wave*, ed. M. C. Clampin, G. G. Fazio, H. A. MacEwen, & J. M. O. Jr., Vol. 8442, International Society for Optics and Photonics (SPIE), 84422R
- Ferruit, P., Bagnasco, G., Barho, R., et al. 2012, in *Space Telescopes and Instrumentation 2012: Optical, Infrared, and Millimeter Wave*, ed. M. C. Clampin, G. G. Fazio, H. A. MacEwen, & J. M. O. Jr., Vol. 8442, International Society for Optics and Photonics (SPIE), 84422O
- Gillon, M., Triaud, A. H. M. J., Demory, B.-O., et al. 2017, *Nature*, 542, 456
- Kempton, E. M.-R., Bean, J. L., Louie, D. R., et al. 2018, *Publications of the Astronomical Society of the Pacific*, 130, 114401
- Kopparapu, R. K., Ramirez, R., Kasting, J. F., et al. 2013, *The Astrophysical Journal*, 765, 131
- Krissansen-Totton, J., Garland, R., Irwin, P., & Catling, D. C. 2018, *The Astronomical Journal*, 156, 114
- Krist, J. E., Balasubramanian, K., Muller, R. E., et al. 2010, in *Space Telescopes and Instrumentation 2010: Optical, Infrared, and Millimeter Wave*, ed. J. M. O. Jr., M. C. Clampin, & H. A. MacEwen, Vol. 7731, International Society for Optics and Photonics (SPIE), 77313J
- Leconte, J., Forget, F., Charnay, B., Wordsworth, R., & Pottier, A. 2013, *Nature*, 504, 268
- Lustig-Yaeger, J., Fu, G., May, E. M., et al. 2023, *Nature Astronomy*
- Mayor, M. & Queloz, D. 1995, *Nature*, 378, 355
- Rieke, G. H., Wright, G. S., Böker, T., et al. 2015, *Publications of the Astronomical Society of the Pacific*, 127, 584
- Rieke, M. J., Kelly, D. M., & Horner, S. D. 2005, in *Cryogenic Optical Systems and Instruments XI*, ed. J. B. Heaney & L. G. Burriesci, Vol. 5904, International Society for Optics and Photonics (SPIE), 590401

Sullivan, P. W., Winn, J. N., Berta-Thompson, Z. K., et al. 2015, *The Astrophysical Journal*, 809, 77

Wunderlich, Fabian, Scheucher, Markus, Grenfell, John Lee, et al. 2021, *AA*, 647, A48

Ringraziamenti

Desidero esprimere la mia più sincera gratitudine a tutte le persone che hanno contribuito alla realizzazione di questa tesi e che mi hanno sostenuto lungo questo percorso. In particolare, desidero ringraziare:

Il mio relatore, il Professor Luca Malavolta, per la sua costante disponibilità e professionalità lungo tutto il progetto di ricerca. La sua passione e i preziosi consigli sono stati fondamentali nel percorso che mi ha portato a completare questa tesi.

La mia famiglia, per il loro affetto incondizionato e il loro incoraggiamento costante. Hanno creduto in me in ogni momento, fornendomi sostegno morale e forza per affrontare e superare ogni sfida.

Jesbol, per il suo amore, il suo sostegno e la sua comprensione. La tua presenza accanto a me è stata una fonte di conforto e ispirazione. Sei stata la luce nei momenti bui e una compagnia gioiosa nelle celebrazioni delle mie vittorie.

I miei amici, per i momenti di svago che hanno reso questo viaggio meno gravoso. La loro presenza, sia nei momenti di stress sia in quelli di celebrazione, ha aggiunto valore a questa esperienza.

Il vostro sostegno è stato cruciale per il successo di questa tesi e vi sono profondamente grato. Ognuno di voi ha lasciato un'impronta indelebile nel capitolo più importante della mia vita.

Con sincera gratitudine,

Andrea Semenzato.